Effects of Synaptic Noise and Filtering on the Frequency Response of Spiking Neurons

Nicolas Brunel,[1] Frances S. Chance,[2] Nicolas Fourcaud,[1] and L. F. Abbott[2]

[1]*LPS, Ecole Normale Supérieure, 24 rue Lhomond, 75231 Paris Cedex 05, France*

[2]*Volen Center and Department of Biology, Brandeis University, Waltham, Massachusetts 02454*

(Received 15 September 2000)

Noise can have a significant impact on the response dynamics of a nonlinear system. For neurons, the primary source of noise comes from background synaptic input activity. If this is approximated as white noise, the amplitude of the modulation of the firing rate in response to an input current oscillating at frequency ω decreases as $1/\sqrt{\omega}$ and lags the input by 45° in phase. However, if filtering due to realistic synaptic dynamics is included, the firing rate is modulated by a finite amount even in the limit $\omega \to \infty$ and the phase lag is eliminated. Thus, through its effect on noise inputs, realistic synaptic dynamics can ensure unlagged neuronal responses to high-frequency inputs.

DOI: 10.1103/PhysRevLett.86.2186 PACS numbers: 87.19.La, 05.40.–a, 87.19.Nn

Neurons in cortical and other neural circuits receive a continuous barrage of synaptic input that acts as a source of noise and makes neuronal responses highly variable (see, e.g., [1]). Noise inputs can also affect other neuronal response characteristics [2–7]. Knight [6] and Gerstner [7] have shown that noise can simplify the dynamics of neuronal firing rates, and that, for some types of noise, the firing rate of a neuron can replicate the time course of an input current, no matter how rapidly it varies. This is rather surprising because the membrane capacitance and resistance of a neuron act as a low-pass filter on the input current. While intriguing, these results are not based on realistic models of the background synaptic input that a neuron receives, but rely instead on simpler noise models. Yet these analyses and the results reported below make it clear that the response dynamics are sensitive to details of the noise model. Here, using a combination of analytic and computational techniques, we examine how synaptic input modeled after that received by a cortical neuron *in vivo* affects the response characteristics of a model neuron.

The integrate-and-fire model we use in this analysis represents the electrical properties of the neuron by parallel resistor (R) and capacitor (C) elements [8]. The basic equation determining the potential V across the cell membrane is

$$\tau_{\mathrm{m}} \frac{dV}{dt} = V_{\mathrm{rest}} - V + I ,$$

where τ_{m} is the time constant of the RC circuit, V_{rest} is the equilibrium or resting potential in the absence of input, and I represents the sum of all inputs to the neuron. Action potentials are generated in the model whenever the membrane potential reaches a threshold value, V_{th}. At this point, the membrane potential is reset to a value V_{reset}. In our analysis, the neural response is specified by a firing rate $r(t)$, which is the probability density for action potentials to occur at time t. To probe the response dynamics of the integrate-and-fire model in the presence of noise, we express the total current as the sum of input and noise terms, $I = I_{\mathrm{in}} + I_{\mathrm{noise}}$, and consider the case of an oscillating input current, $I_{\mathrm{in}} = I_0 + I_1 \cos(\omega t)$. I_{noise} represents the combined effect of large numbers of excitatory and inhibitory synaptic inputs. Biological synapses modify the conductances of their neuronal targets rather than simply injecting current. We have performed simulations that include synaptic effects on conductance and find no appreciable differences from the results reported here using the more analytically tractable approximation of synaptic currents.

We characterize the firing rate by its time average, r_0, and by the amplitude and phase of its Fourier transform at the frequency ω, $r_1(\omega)$, and $\phi(\omega)$. This is equivalent to approximating the firing rate as $r(t) = r_0 + r_1(\omega)\cos[\omega t + \phi(\omega)]$. Provided that $r_1(\omega) \leq r_0$, the firing rate is well fit by this expression, except near the resonances that occur at low noise levels.

Knight [6] showed that, in the absence of noise, the firing rates of integrate-and-fire neurons display resonances when $\omega/2\pi$ is an integer multiple of r_0. These distort the response of the system relative to the input. Knight also computed the firing rate for a simplified noise model, based on choosing a random threshold after each spike, and showed that noise decreased the size of, or eliminated, the resonant peaks. For some noise conditions, Knight found that $r_1(\omega)$ was independent of frequency and $\phi(\omega) = 0$. Gerstner [7] obtained related results in a more general formulation.

The noise input we analyze is generated by action potentials carried by thousands of afferent fibers, and it can be modeled as a high-rate Poisson process. Because of the high rate, this is well approximated by a Gaussian white-noise source. Synapses transmit input action potentials with a very rapid rise time but a slower exponential decay with a time constant τ_{s}. This has the effect of low-pass filtering the input noise. Thus, we write

$$\tau_{\mathrm{s}} \frac{dI_{\mathrm{noise}}}{dt} = \eta(t) - I_{\mathrm{noise}} ,$$

where $\eta(t)$ is a Gaussian white-noise random variable satisfying $\langle \eta(t) \rangle = 0$ and $\langle \eta(t)\eta(t') \rangle = \sigma^2 \delta(t - t')\tau_{\mathrm{m}}$. We

 0031-9007/01/86(10)/2186(4)$15.00

use the parameter σ, which is in mV units, to characterize the amplitude of the noise.

When $\tau_s = 0$ (white noise), the probability density for the membrane potential of the neuron at time t, $P(V,t)$, is described by the Fokker-Planck equation (see, e.g., [9]),

$$\tau_m \frac{\partial P}{\partial t} = \frac{\sigma^2}{2} \frac{\partial^2 P}{\partial V^2} + \frac{\partial}{\partial V}[V - I_{in}(t) - V_{rest}]P. \quad (1)$$

The firing rate is proportional to the flux $\partial P(V,t)/\partial V$ when an absorbing boundary condition is imposed at the firing threshold V_{th},

$$r(t) = -\frac{\sigma^2}{2\tau_m} \frac{\partial P(V,t)}{\partial V}\bigg|_{V=V_{th}},$$

with $P(V_{th},t) = 0$. This flux is returned at the reset potential so, in the limit $\epsilon \to 0$, $P(V_{reset} - \epsilon, t) = P(V_{reset} + \epsilon, t)$ and

$$\frac{\partial P(V,t)}{\partial V}\bigg|_{V=V_{reset}-\epsilon}^{V=V_{reset}+\epsilon} = -\frac{2r(t)\tau_m}{\sigma^2}.$$

The time-independent solution of Eq. (1) for constant input ($I_1 = 0$) has been known for a long time (see, e.g., [10]). More recently, methods were introduced in [11] that can be used to determine the solution for an oscillating input, $I_{in} = I_0 + I_1 \cos(\omega t)$, when I_1/I_0 is small. The result of this calculation is

$$r_1(\omega)e^{i\phi(\omega)} = \frac{r_0 I_1}{\sigma(1 + i\omega\tau_m)} \times \left(\frac{\frac{\partial U}{\partial y}(y_t,\omega) - \frac{\partial U}{\partial y}(y_r,\omega)}{U(y_t,\omega) - U(y_r,\omega)} \right), \quad (2)$$

where $y_t = (V_{th} - I_0 - V_{rest})/\sigma$, $y_r = (V_{reset} - I_0 - V_{rest})/\sigma$, and U is given in terms of combinations of hypergeometric functions [12]

$$U(y,\omega) = \frac{e^{y^2}}{\Gamma[(1 + i\omega\tau_m)/2]} M\left(\frac{1 - i\omega\tau_m}{2}, \frac{1}{2}, -y^2\right) + \frac{2ye^{y^2}}{\Gamma(i\omega\tau_m/2)} M\left(1 - \frac{i\omega\tau_m}{2}, \frac{3}{2}, -y^2\right). \quad (3)$$

Results of the analytic computation for $\tau_s = 0$ are illustrated in Fig. 1. These are exact only in the limit $I_1/I_0 \to 0$. To explore larger I_1/I_0 we determined the modulation amplitude and phase of the firing rate of an integrate-and-fire neuron by computer simulation. The results, shown in Fig. 1, indicate that the analytic expression holds to a high degree of accuracy over the entire range of I_1 for which the firing rate remains in the interval $[0, 2r_0]$ (when the modulation becomes larger and the firing rate becomes zero in a part of the cycle the dynamics of the model change considerably).

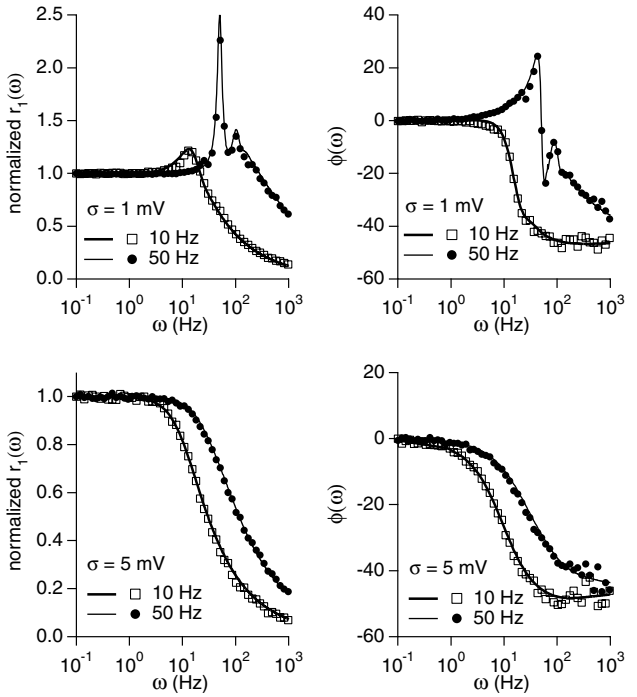

FIG. 1. Response amplitude and phase for $\tau_s = 0$. Solid lines indicate the analytical predictions [Eq. (2)] and symbols represent simulation results. Throughout we use $\tau_m = 20$ ms, $V_{th} = -54$ mV, $V_{reset} = -60$ mV, and $V_{rest} = -74$ mV. The value of σ is indicated in the legend of each panel. For the simulations, I_{in} was adjusted so that $r_1 = r_0$ with the value of r_0 given in the legend. This corresponds to an input regime where I_1/I_0 is no longer small. Modulation amplitudes (left panels) are reported as $r_1(\omega)/r_1(0.1)$, i.e., normalized to the amplitude for 0.1 Hz.

Several features are apparent from both the analytic and simulation results for $\tau_s = 0$. As found in [6], the amplitude of the response modulation for low-noise levels ($\sigma = 1$ mV; upper panels of Fig. 1) peaks at input frequencies that are integer multiples of r_0. The resonance peaks become less pronounced as r_0 decreases or σ increases and are absent at high-noise levels ($\sigma = 5$ mV; lower panels of Fig. 1). In all cases, the modulation amplitude $r_1(\omega)$ goes to zero as $1/\sqrt{\omega}$ for large ω. Outside of the resonance regions, there is a phase lag in the response [$\phi(\omega) < 0$] that approaches $-45°$ as $\omega \to \infty$. Thus, the distortion in the response relative to the input caused by the resonances can be eliminated if a sufficient amount of unfiltered white noise ($\tau_s = 0$) is added to the model. However, white noise does not allow the firing rate to be modulated at arbitrarily high input frequencies, and a phase lag is always present in the high-frequency response.

The synaptic noise received by neurons *in vivo* is not white because τ_s is in a range from a few to tens or even hundreds of ms for biological synapses. When the white noise is filtered, the analytic calculations are significantly more complex [13,14]. It is no longer possible to find an exact solution for the stationary probability density and firing rate for constant input current. However, calculations can be done in the limit $\tau_s \ll \tau_m$, and, in particular,

the first correction to the stationary firing rate, of order $\sqrt{\tau_s/\tau_m}$, can be computed in that limit [15]. Furthermore, the same small amplitude oscillation calculation reported above can be performed in this limit for the case $I_{in} = I_0 + I_1 \cos(\omega t)$.

With filtered noise ($\tau_s > 0$), the firing rate is determined by a distribution $P(y, z, t)$ that depends on $y = (V - I_0 - V_{rest})/\sigma$ and the additional synaptic current variable

$$z = \sqrt{\frac{\tau_s}{\tau_m}} \left(\frac{I_{noise} + I_1 \cos(\omega t) + V_{rest} - V_{th}}{\sigma} \right).$$

This definition is chosen because it simplifies the boundary conditions and assures that z has a finite variance in the limit $\tau_s/\tau_m \to 0$. $P(y, z, t)$ obeys the equation

$$\tau_s \frac{\partial P}{\partial t} = \frac{1}{2} \frac{\partial^2 P}{\partial z^2} + \frac{\partial (zP)}{\partial z} + \sqrt{\frac{\tau_s}{\tau_m}} \left\{ \left[y_t - \frac{I_1}{\sigma} (\cos(\omega t) - \omega \tau_s \sin(\omega t)) \right] \frac{\partial P}{\partial z} - z \frac{\partial P}{\partial y} \right\} + \frac{\tau_s}{\tau_m} \frac{\partial (y - y_t) P}{\partial y}.$$

The boundary condition on the line $y = y_t$ is $\nu(z, t) = zP(y_t, z, t)/\sqrt{\tau_s \tau_m}$ for $z > 0$, and $P(y_t, z, t) = \nu(z, t) = 0$ for $z < 0$, where $\nu(z, t)$ corresponds to the probability flux in the y direction at the voltage threshold. The condition that the flux has to be zero on the half line $z < 0$ is related to the fact that when a neuron fires, the time derivative of the potential and hence z can only be positive. The prescription of zero probability density on a half line is the main factor that significantly complicates the analysis. The firing rate at time t is

$$r(t) = \int_{-\infty}^{\infty} dz\, \nu(z, t).$$

On the line $y = y_r$, we have $z + \sqrt{\tau_s/\tau_m}(y_t - y_r)/[P(y_r + \epsilon, z, t) - P(y_r - \epsilon, z, t)] = zP(y_t, z, t)$ for $z > 0$, and $P(y_r + \epsilon, z, t) = P(y_r - \epsilon, z, t)$ for $z < 0$. We then write $P = P_0(y, z) + \mathrm{Re}[P_1(y, z, \omega) e^{i\omega t}]$. When $I_1/I_0 \ll 1$, the Fokker-Planck equation can be linearized around the stationary solution P_0, r_0. Solutions to this equation to leading orders in $\sqrt{\tau_s/\tau_m}$ can be found in both the low- ($\omega \sim 1/\tau_m$) and high- ($\omega \gg 1/\tau_s$) frequency limits. In the high-frequency limit, we obtain

$$\lim_{\omega \to \infty} P_1(y, z, \omega) = -\frac{I_1}{\sigma} \sqrt{\frac{\tau_s}{\tau_m}} \frac{\partial P_0}{\partial z}(y, z),$$

and

$$\lim_{\omega \to \infty} r_1(\omega) e^{i\phi(\omega)} = \frac{I_1}{\sigma \tau_m} \int_{-\infty}^{\infty} dz\, P_0(y_t, z).$$

The stationary distribution at threshold, $P_0(y_t, z)$, can be calculated along the lines of [13–15]. It is of order $\sqrt{\tau_s/\tau_m}$ for small τ_s/τ_m, and

$$\lim_{\omega \to \infty} r_1(\omega) e^{i\phi(\omega)} = \frac{A r_0 I_1}{\sigma} \sqrt{\frac{\tau_s}{\tau_m}}, \qquad (4)$$

where

$$A = \sqrt{2} \left| \zeta\left(\frac{1}{2}\right) \right| - \frac{1}{\sqrt{2}} \sum_n \frac{N(\sqrt{n}) n^{(n-1)/2} e^{-n/2}}{n!} \approx 1.3238,$$

where ζ is Riemann's zeta function [12], and

$$N(\sqrt{n}) = \prod_{k=1}^{\infty} \left(1 + \sqrt{\frac{n}{k}}\right) e^{-2\sqrt{n}(\sqrt{k} - \sqrt{k-1})} \left(\frac{k+1}{k}\right)^{n/2}.$$

The analytic results show that filtering of the noise by the synaptic dynamics dramatically changes the high-frequency behavior of $r_1(\omega)$. In contrast to the white-noise case, $r_1(\omega)$ now approaches a finite limit as $\omega \to \infty$. Furthermore, the high-frequency limit of $\phi(\omega)$ is zero for any positive τ_s. This means that the neuronal firing rate can be modulated by an oscillating input up to arbitrarily high frequencies without a phase lag when $\tau_s > 0$.

Equation (4) indicates that the high-frequency limit of the response increases with larger values τ_s, but the calculation is only valid for $\tau_s \ll \tau_m$. To explore larger values of τ_s/τ_m, we performed simulations of the integrate-and-fire model with filtered white-noise input (Fig. 2). The simulation results indicate that the high-frequency modulation amplitude continues to rise as τ_s is increased

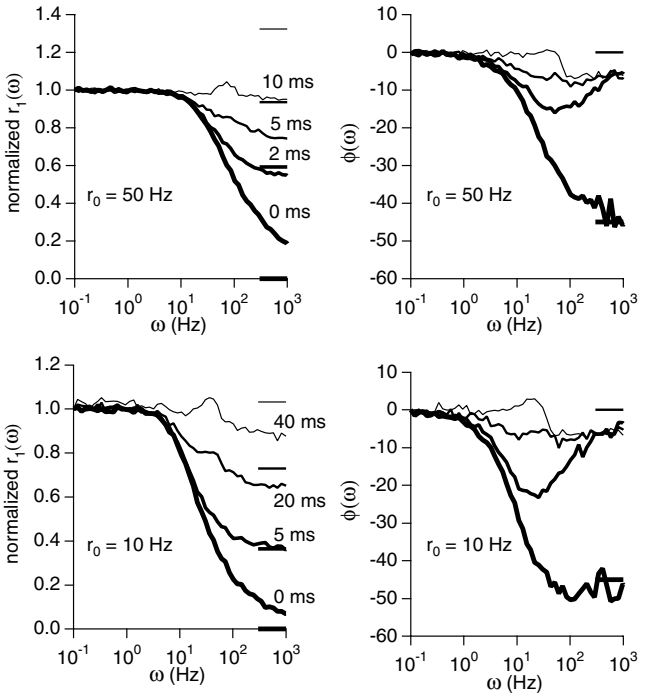

FIG. 2. Response amplitude and phase for $\tau_s > 0$, and $\sigma = 5$ mV. Traces represent simulation results for the values of τ_s indicated to the right of each trace in the left panels showing $r_1(\omega)/r_1(0.1)$. The ticks on the right of all four panels indicate the high-frequency limit predicted by Eq. (4). For the phase plots (right panels), the value of τ_s is the same as for the amplitude trace to the left with the corresponding thickness. For the upper and lower panels $r_0 = 50$ Hz and 10 Hz, respectively, and in both cases $r_1 = r_0$. The thick curves correspond to the simulation data in the lower two panels of Fig. 1.

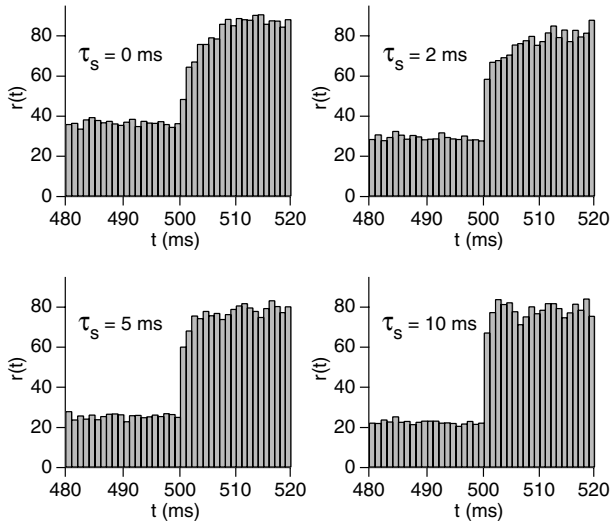

FIG. 3. Firing rate in response to a step in the input current. Histograms show the firing rate $r(t)$ of the model integrate-and-fire neuron, with τ_s as indicated, to a step of input current at 500 ms. Firing rates were computed by counting action potentials in 1 ms bins.

until the high- and low-frequency modulation amplitudes are roughly equal. The phase of the response also tends to zero as τ_s is increased. If τ_s is increased still further, so that $2\pi r_0 \tau_s$ is of order 1 or greater, the resonances that were removed by the high-noise condition when $\tau_s = 0$, return. This is due to the filtering of the white noise in the frequency range corresponding to the average firing rate. Note from Fig. 2 that a larger τ_s value is required to achieve an approximately flat response amplitude for smaller values of r_0. The analytic results of Eq. (4) agree fairly well with the highest frequency simulations. Similar results were obtained in the low-noise case, that is, increasing τ_s caused a progressive flattening of the response amplitude at high frequency. The resonance phenomenon is still present in the low-noise results, no matter what value of τ_s is used, and the analytic results of Eq. (4) are considerably less accurate unless $\tau_s \ll \tau_m$.

Our study interpolates between two previously investigated limits. In the large τ_s limit, the input model becomes a "slow" noise model (i.e., the cutoff frequency of the noise is of the same order of magnitude as the firing rate of the neuron), and our results become comparable to that of earlier slow noise models [6,7]. At the other extreme, with "fast" white-noise input, our results are also consistent with previous results using a different type of fast noise, escape noise [7].

We have seen that synaptic dynamics can have a significant impact on neuronal responses to current inputs with high-frequency components. Increasing the synaptic time constant of the noise inputs enhances the high-frequency response. Figure 3 illustrates the effect this has on the responses of an integrate-and-fire neuron to an instantaneous step in the input current. As τ_s is increased from 0 to 10 ms, the response of the neuron gets more and more rapid and, for $\tau_s = 10$ ms, it follows the input current almost instantaneously.

Analysis of neuronal response variability indicates that the noise present *in vivo* roughly matches the higher of the noise levels used in our analysis ($\sigma = 5$ mV) [16]. Typical fast excitatory and inhibitory synapses (AMPA and $GABA_A$ synapses) have time constants in the range of 2 to 5 ms (see, e.g., [17]), large enough to significantly affect response dynamics. Interestingly, $\tau_s = 5$ ms is at the lower range of values for which an extremely rapid response to a step of input current is obtained (Fig. 3). While increasing τ_s to even larger values for noise inputs might further enhance high-frequency responses, this would also lead to stronger resonance phenomena. An interesting possibility in this regard is that signal changes are mainly due to fast excitatory synapses of the AMPA type, while noise is mainly implemented through slower GABA synapses. Thus, the observed values of synaptic time constants may be tuned to achieve both rapid and undistorted responses to time-varying inputs.

[1] F. M. Rieke, D. Warland, R. de Ruyter van Steveninck, and W. Bialek, *Spikes: Exploring the Neural Code* (MIT, Cambridge, MA, 1997).
[2] H. Spekreijse and H. Oosting, Kybernetik **7**, 1461–1472 (1970).
[3] D. J. Amit and M. V. Tsodyks, Network **2**, 259–274 (1991).
[4] D. J. Amit and M. V. Tsodyks, Network **3**, 121–138 (1992).
[5] M. Carandini, F. Mechler, C. S. Leonard, and J. A. Movshon, J. Neurophysiol. **76**, 3425–3441 (1996).
[6] B. W. Knight, J. Gen. Physiol. **59**, 734–766 (1972).
[7] W. Gerstner, Neural Comput. **12**, 43–89 (2000).
[8] H. C. Tuckwell, *Introduction to Theoretical Neurobiology* (Cambridge University Press, Cambridge, 1988).
[9] H. Risken, *The Fokker Planck Equation: Methods of Solution and Applications* (Springer-Verlag, Berlin, 1984).
[10] L. M. Ricciardi, *Diffusion Processes and Related Topics on Biology* (Springer-Verlag, Berlin, 1977).
[11] N. Brunel and V. Hakim, Neural Comput. **11**, 1621–1671 (1999).
[12] M. Abramowitz and I. A. Stegun, *Tables of Mathematical Functions* (Dover Publications, New York, 1970).
[13] P. S. Hagan, C. R. Doering, and C. D. Levermore, SIAM J. Appl. Math. **49**, 1480–1513 (1989).
[14] M. M. Klosek and P. S. Hagan, J. Math. Phys. (N.Y.) **39**, 931–953 (1998).
[15] N. Brunel and S. Sergi, J. Theor. Biol. **195**, 87–95 (1998).
[16] T. W. Troyer and K. D. Miller, Neural Comput. **9**, 971–983 (1997).
[17] A. Destexhe, Z. F. Mainen, and T. J. Sejnowski, in *Methods in Neuronal Modeling,* edited by C. Koch and I. Segev (MIT, Cambridge, MA, 1998), 2nd ed.